Development of a sensitive multiplexed open circuit potential system for the detection of prostate cancer biomarkers

Lai Chun Caleb Wong, Pawan Jolly, Pedro Estrela *

Department of Electronic & Electrical Engineering, University of Bath, Bath BA2 7AY, United Kingdom

*Corresponding author: Department of Electronic & Electrical Engineering,
University of Bath,
Claverton Down, Bath, BA2 7AY, United Kingdom
E-mail: P.Estrela@bath.ac.uk
Phone: +44-1225-386324

Abstract

We report the development of a sensitive label-free, cost-effective detection system with simultaneous multi-channel measurement of open circuit potential (OCP) variations for the detection of prostate specific antigen (PSA). We demonstrate a significant increase of 600 times in the sensitivity as compared to the reported literature. To accurately measure OCP variations, a complete monolithic field-effect transistor (FET)-input ultra-low input bias current instrumentation amplifier is used to form the electronic circuit to measure the variation between a working electrode and a reference electrode. This amplifier electronic system setup provides a differential voltage measurement with high input impedance and low input bias current. Since no current is applied to the electrochemical system, a true and accurate measurement of the variation can be performed. This is the first report on the use of DNA aptamers with OCP system where we employed a DNA aptamer against PSA. An optimised ratio of anti-PSA DNA aptamer with 6-mercapto-1-hexanol (MCH) was used to fabricate the aptasensor using gold electrodes. The electrodes are hosted in a cell with an automated flow system. A wide range of concentrations of PSA (0.1 ng/mL to 100 ng/mL) were injected through the system. The sensor could potentially differentiate 0.1 ng/mL PSA from blank measurement, which is well below the required clinical range (>1 ng/mL). The sensor was also challenged with 4% human serum albumin and human kallikrein2 as control proteins where the sensor demonstrated excellent selectivity. The developed system can be further generalised to various other targets using specific probes.

Keywords: aptamer, prostate cancer diagnosis, prostate specific antigen, open circuit potential

1. Introduction

Label-free technologies have gained a high interest in the past decade for the development of biosensors that could achieve high throughput screening capabilities. In a recent report, the global label-free detection market was valued at USD 1.22 Billion in 2015, and expected to reach USD 2.13 Billion by 2020, at a compound annual growth rate of 11.86% from 2015 to 2020 [1]. Label-free technologies provide opportunities for probing biomolecular interactions without spatial interference, steric hindrance, auto-fluorescent and quenching effects of labels. Freeing from a preparatory step for labelling (dyes, tags, or specialized reagents), increasing the throughput screening targets at a single time and, consequently, lowering the overall cost of the system. Conventional label-based technologies, however, are usually labour intensive, time consuming and cumbersome, resulting in a higher cost when compared to label-free technologies. Thus an increasing amount of studies based on label-free detection technologies have been made with different detection methods [2-8]. In the field of electrochemical sensing, different detection techniques have been introduced to use label-free technologies, such as electrochemical impedance spectroscopy (EIS) and differential pulse voltammetry (DPV). However, these techniques still rely on the use of redox markers to distinguish the reaction on the biolayer, which has put pressing needs on the development of novel technologies. To take up such a challenge, an open circuit potential (OCP) detection technique finds its right application.

OCP variations can be used to detect biomolecular interactions on a metal electrode. This potentiometric detection technique is the direct measurement of potential

variations brought about by changes in the net charge or capacitance on the biolayer. The variation during binding/attachment of biomolecules can then be monitored in real time. Direct OCP measurements cannot be achieved in an accurate way with standard potentiostats due to their circuit architecture. To date, there has been only few reports on the use of OCP as a detection technique. For instance, Estrela *et al.* [9] first demonstrated that electrical detection of protein interactions can be achieved by the direct measurement of OCP variations through an instrumentation amplifier using a single channel for detection. Such system presents an alternative to the use of metal-gate field effect transistors (BioFET), where OCP variations on the metal gate cause a shift on the threshold voltage of the BioFET [10]. Mello *et al.* [11] demonstrated the use of instrumentation amplifiers for pH sensing using polyaniline films and Harb *et al.* [12] discussed the relations of OCP to nanocomposites.

For many biosensing applications there has been increasing interest in the use of aptamers. Although antibodies have dominated commercial adoption, aptamers provide a wide range of advantageous properties such as long-term stability, affordability and ease of development compared to antibodies [13,14]. They can also be regenerated without loss of integrity or selectivity [15]. There are plenty of reports covering the development of aptasensors based on different detection techniques from optical to electrochemical routes. However, in the niche of potentiometric sensors, OCP had still not been investigated.

We therefore present for the first time a sensitive label-free detection flow system with simultaneous multi-channel measurement of OCP variations for the detection of prostate specific antigen (PSA) as a case study. PSA is a 30 kDa protein found in blood which is the sole biomarker currently used for prostate cancer (PCa). PCa is the most commonly diagnosed cancer amongst men in Europe and the United States, and is the second-highest cause of cancer-related morbidity worldwide [16]. Changes in PSA levels in the blood can be used for PCa screening with levels higher than the cut-off level of 4 ng/mL prompting biopsy procedures to be considered [16-19].

We have used anti-PSA aptamer to detect different concentrations of PSA using the OCP technique. We have previously demonstrated the optimisation of different surface chemistries for PSA aptamer-based impedimetric sensors; although high sensitivity has been obtained for novel approaches, we note that for a simple aptamer / mercaptohexanol self-assembled monolayer, a detection limit of 60 ng/mL has been obtained [20], which is much higher than the clinical range. In the present study, we have used a similar approach to prepare electrode surfaces with DNA aptamers and detected PSA in real time. A very low detection of 0.1 ng/mL which is 600 times increased sensitivity than using electrochemical impedance spectroscopy as a detection technique. The aptasensor developed demonstrated a good selectivity when challenged with control proteins such as human Kallikrien 2 (hK2) and human serum albumin (HSA). We present a simple instrumentation system with a sensitive detection limit that could be easily generalised to other probes for the detection of various other biomarkers and easily realise multiplexed detection.

2. Materials & Methods

2.1. OCP electronic design

The amplifier electronic system setup provides a differential voltage measurement with high input impedance and low input bias current. Since no current is applied to the electrochemical system, a true and accurate measurement of the variation can be performed. To accurately measure OCP variations, a complete monolithic FET-input ultra-low input bias current instrumentation amplifier INA116 (Texas Instruments, USA) is used to form the electronic detection circuit, measuring the variations between the working electrode and the reference electrode (see Figure 1). A Pt wire is used to ground the electrolyte. A stable and isolated ±15 V power circuit supplies the power specifically for the instrumentation amplifier to improve the working condition of the amplifier to the maximum performance. A DC/DC converter MCA05D15S (Multicomp, USA) was selected to supply an isolated ±15 V (setpoint accuracy ±3%) with a maximum peak-to-peak ripple of 75 mV measured with a 20 MHz bandwidth. This power supply and connected power lines are separated from all other signal lines or power lines of other electronics. The differential measurement outputs (V_0) from the amplifiers are then passed into an analog-to-digital converter (ADC).

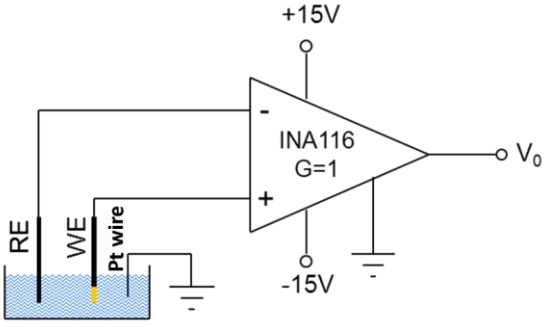

Fig. 1 Schematic of the basic design of a single channel OCP measurement system. WE is the working electrode; RE the reference electrode; the Pt wire is grounding the solution.

The overall closed-loop gain (G) of the instrumentation amplifier can be described as

$$G = 1 + \frac{50k\Omega}{R_G} \quad (1)$$

where R_G is the single gain-setting external resistor. To eliminate any further errors that can be caused by the mismatch of multi-channel electronic components, the amplifiers of all channels are set to unity gain differential configuration (G = 1).

A 24-bit, 4-channel, simultaneous-sampling, sigma-delta analog-to-digital converter (ADC) MAX11040K (Maxim Integrated, USA) is selected for sampling the differential outputs of the instrumentation amplifiers, which are the OCP analog signals. The differential analog input range is ±2.2 V when using the internal reference voltage (V_{REFIO}), which is well within the input OCP signal. Code transitions occur halfway between successive integer least significant bit (LSB) values with 1 LSB = (0.88 x V_{REFIO}) x 2/16,777,216 in 24-bit mode. This ADC allows high resolution and simultaneous sampling of 4 channels on its own (see Figure 2) and up to 32 channels by using a built-in cascade feature to synchronize as many as eight devices on a single serial interface. The simplicity of the device allows reading data from all the cascaded devices using a single command, with the eight devices effectively operating as one device. In the current design, a single ADC is used, which gives a 4-channel simultaneous-sampling system.

An Arduino UNO (Arduino, USA) is used as the main controller. Stacked on top with a module board that hosted the INA116 instrumentation amplifiers and the MAX11040K ADC. Digital data is outputted from the ADC through a microprocessor into a computer, and monitored through a LabVIEW program in real time.

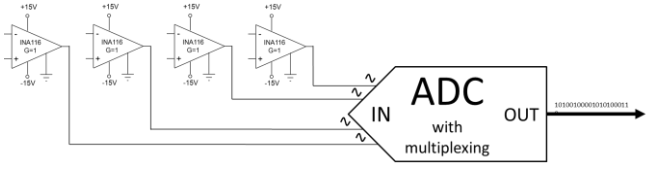

Fig. 2 Schematic of the multiplexed OCP detection circuit constructed with four INA116 instrumentation amplifiers and one MAX11040K ADC.

2.2. Electrochemical characterization

OCP measurements were carried out using the custom made electronic measurement system based on the INA116 ultra low input bias current instrumentation amplifiers design. The simultaneous measurement setup, illustrated in Figure 3, consisted of a linear array of four working electrodes with a radius of 2.0 mm, an Ag/AgCl (3 M NaCl) reference electrode (BASi, USA), and a platinum wire (ALS Co., Japan) for grounding the solution in the electrochemical cell. The working electrode linear array was prepared in-house by thermal evaporation (BOC Edwards, USA) with 20 nm chromium and 100 nm gold on a glass slide. The OCP was measured in a solution of 10 mM phosphate buffer (PB) (pH 7). The reference electrode was connected via a salt bridge filled with the same 10 mM PB (pH 7) solution. The OCP was recorded in real time; solutions of PSA from the lowest to the highest concentrations were injected into the flow cell. A multiplexed design of four working electrodes was measured at the same time through four different channels for the potential changes, by using a common reference electrode. Binding studies were carried out under a flow rate of 100 µl/min using a peristaltic pump (323-Du, Watson Marlow, UK) and an in-house built polytetrafluoroethylene (PTFE) flow cell with an inner chamber of approximate dimensions 25 × 8 × 5 mm^3 (length × width × height) and an internal volume of 1 ml.

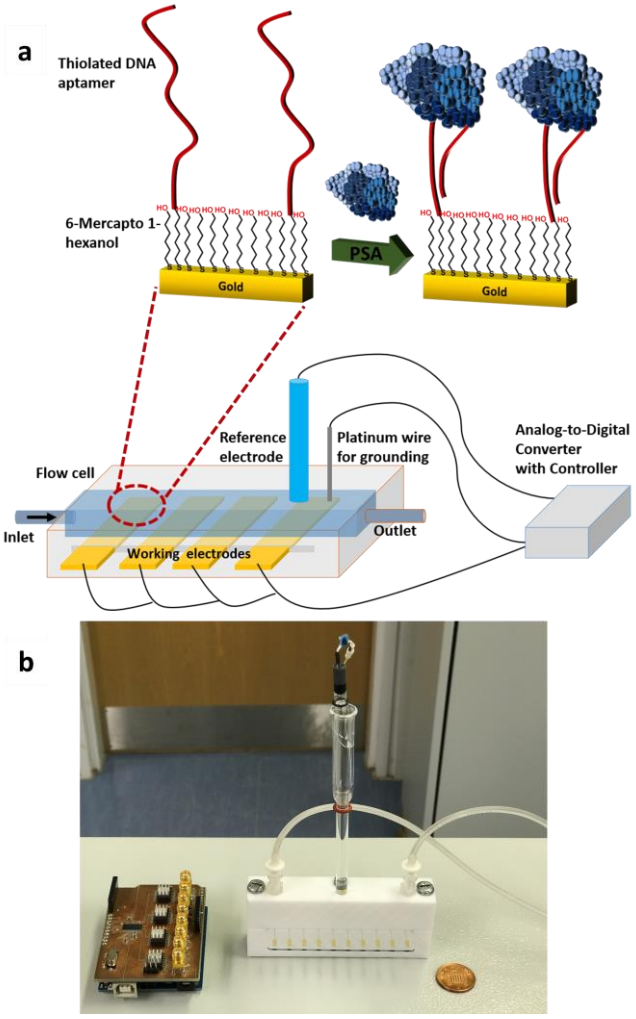

Fig. 3 (a) An illustration of the whole OCP system setup, including the fabricated PSA aptasensor loaded in a flow cell. **(b)** A photo of the flow cell and circuit board.

2.3. Fabrication of PSA aptasensor

Experiments with PSA aptamer were performed using the gold evaporated electrodes following a previously reported protocol [20-21]. Briefly, the clean gold electrodes were exposed to 5 µl of immobilization solution containing thiolated DNA aptamer and 6-mercapto-1-hexanol (MCH, Sigma, UK) for 16 h in a humidity chamber. An optimized 0.5% DNA aptamer mole fraction to total thiol was used to fabricate the biosensor [21]. A high concentration of MCH (10 mM) was prepared in pure ethanol which was then diluted in 10 mM PB (pH 7) to the required working concentrations. Prior to addition of MCH, DNA aptamers were heated to 95 °C for 10 min followed by gradual cooling over 30 min to room temperature [19]. After immobilization, the electrodes were rinsed with excess MilliQ water to remove unattached thiols. In order to ensure complete thiol coverage of the gold surface, the electrodes were thereafter backfilled with 1 mM MCH for 1 h. The electrodes were then rinsed with MilliQ water and placed in 10 mM PB (pH 7) for stabilization.

2.4. Binding studies

The fabricated DNA aptamer modified electrodes were hosted in a cell with an automated flow system. Injections of analyte were performed in 15 minute intervals under a flow rate of 100 µl/min. Different concentrations of PSA from 0.1 ng/mL to 100 ng/mL were prepared in 10 mM PB (pH 7) from stock solutions. Control proteins such as 100 ng/ml hK2 and 66 mg/ml HSA were also prepared in 10 mM PB (pH 7).

3. Results and discussion

3.1. Real time OCP measurements

By using a potentiostat for the measurement of OCP, the circuit architecture applies a very small current into the electrochemical system, and measures the response from the electrochemical system in order to obtain the OCP. Therefore, these systems are not measuring in true open circuit. The use of carefully selected instrumentation amplifiers enables a direct and precise measurement of OCP variations. With this design, no current is applied to the electrochemical system when measuring the OCP and therefore effects that can be caused by passing current through the electrochemical interface can be eliminated.

The current design of the system is a stackable electronic design, with one main controller as the base board. Each module boards have 4 channels for OCP sensing. Extra boards of the INA116 instrumentation amplifiers circuit can be stacked on top of each other, increasing the system capability of simultaneous detection from 4 channels to 32 channels. This can be done as the expansion module board communicates on a single serial interface with the controller. In addition, extra devices are allowed to the system by connecting through extra serial interfaces, allowing the system to be expanded into a high-channel multiplexed OCP measurement setup.

The OCP data was monitored by a computer in real time for live display and recording. Every step of the measurement is illustrated through a voltage (OCP) *vs* time graph. Thus, even the smallest changes can be viewed in real time during the experiment. The data is recorded into a table with timestamp and OCP value and saved in a spreadsheet format. Variations of the OCP values show the binding activity of the biomolecules, and further analysis such as dose response can be obtained through calculation and comparison analysis.

Figure 4 shows real time OCP data for the fabricated aptasensor upon injection of different concentrations of PSA in four separate channels of the linear array of electrodes. The OCP value decreases for increasing concentrations of PSA (starting from 0.01 ng/ml), until it reaches saturation at around 20 ng/ml ($\Delta V_{OCP} \sim$ -3 mV). As a control, samples containing the same volume of buffer without any PSA were also injected into the cell; no significant further variations in OCP were observed, indicating the variations measured are due to binding of PSA. It is worth mentioning that spikes in the measurements are observed when buffer or PSA sample enters the chamber but the values stabilise after 15 min. As shown in the inset of Figure 4, upon injection of buffer, the OCP returns to its original value. All four channels give identical responses to both PSA and buffer injections.

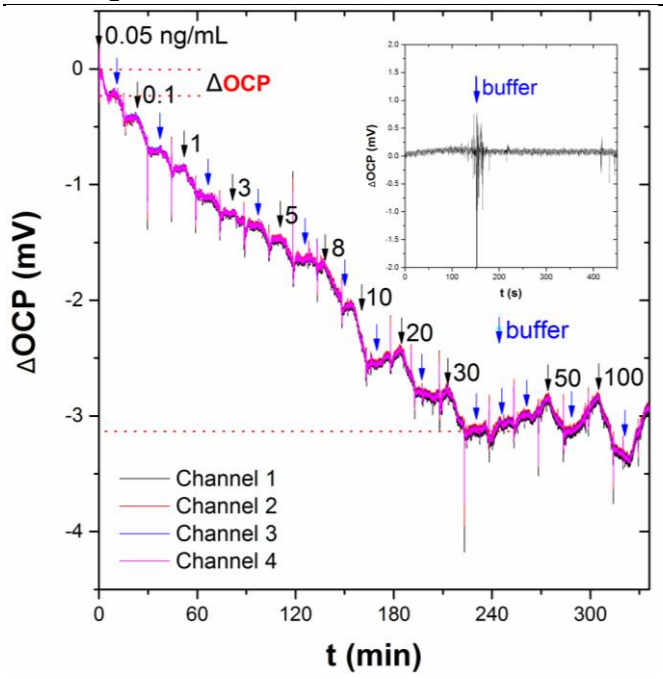

Fig. 4 A typical OCP behaviour of the aptasensor with the response of consecutive injections of different concentrations of PSA (black arrows) and rinsing buffer (blue arrows) on four separate electrodes of the array. The numbers next to the black arrows indicate the PSA concentrations injected. The inset shows the initialization of the OCP measurement with an injection of buffer (blank solution).

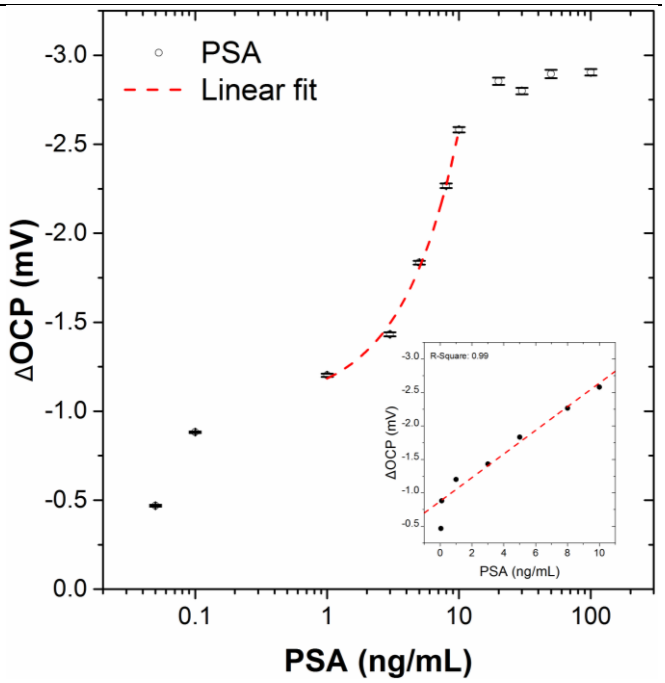

Fig. 5 Dose response of the aptasensor. The points represent the average for 4 channels. The line represents a linear fit to the points between 1 and 10 ng/ml (as shown in the inset using a linear scale).

3.2. Analytical and selectivity performance

A dose response was obtained using all the four channels and is presented in Figure 5. An OCP signal change of -0.880 ± 0.005 mV is observed for 0.1 ng/ml of PSA, decreasing down to -2.850 ± 0.020 mV for 20 ng/ml. Such a decrease in the OCP signal could be attributed to the combined effect of folding of DNA aptamer and the charge of PSA at pH 7. Upon binding of PSA to the immobilised DNA aptamer, the DNA aptamer undergoes a change in conformation causing more negative charges closer to the electrode surface. It is likely that the PSA is either neural or negatively charged depending upon the amount of glycosylation sites. Further injections of PSA do not change this saturation signal. A linear response is obtained from 0.1 ng/ml to 10 ng/ml with an R^2 value of 0.99. The sensor can differentiate 0.1 ng/ml from blank measurements, which is well below the required clinical range (>1 ng/ml).

The sensor was further challenged with two control proteins: human serum albumin (HSA, 4%) and human Kallikrein2 (hK2, 100 ng/mL). hK2 is another serine protease from the same kallikrein family as PSA and was chosen as a stringent control protein since is it shares 80% homology with PSA. Although the levels of hK2 in clinical samples are 100 fold lower than that of PSA, a much higher concentration of 100 ng/ml of protein was used to stringently evaluate the aptamer based detection of PSA [22]. A negligible change with hK2 (-0.174 ± 0.025 mV) was observed as compared to the signal change from PSA with same concentration (-2.900 ± 0.018 mV) – see Figure 6. This clearly indicates the specificity of the aptamer towards PSA. As a further control, 4% HSA (~66 mg/ml) was used since it is a major constituent of blood. A change of +1.100 ± 0.024 mV was observed with HSA in the opposite direction as of PSA. Such a signal change with HSA could be attributed to non-specific interaction of HSA with the SAM. A similar response has been previously reported for impedance PSA aptasensors [20-21].

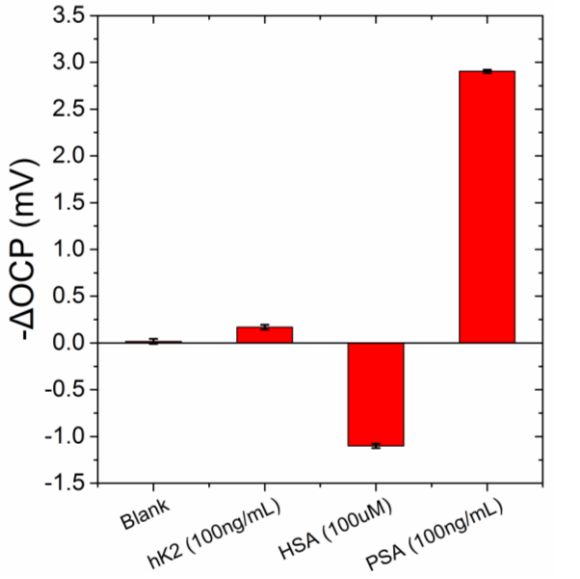

Fig. 6 A comparison of response with blank, hK2 (100 ng/ml), HSA (66000 ng/ml) and PSA (100 ng/ml) fabricated sensors.

4. Conclusions

We have presented a sensitive label free, cost effective OCP system that can be used to develop sensitive aptasensors. In its present configuration, with one instrumentation amplifier per channel and one ADC per 4 channels, the circuitry costs around $50 per 4 channels using off-the shelf components, making the system an attractive cost effective alternative to other electrochemical systems. The aptasensor developed for PSA using this OCP detection technique demonstrated a 600 times increased sensitivity with similar aptasensor using electrochemical impedance spectroscopy. The sensor displayed good selectivity when challenged with stringent control proteins. PSA was used as case study to show the applicability of the technique and the robustness of the multichannel approach. This strategy can be easily adopted for the detection of a wide range of biomarkers in a multiplexed platform using not only aptamers but also other receptor molecules such as peptides, antibodies and lectins.

Acknowledgements

P.J. was funded by the European Commission Seventh Framework Programme through the Marie Curie Initial Training Network PROSENSE (Grant no. 317420, 2012–2016)

References

[1] marketsandmarkets.com, "Label-Free Detection Market by Technology (Surface Plasmon Resonance, Bio-Layer Interferometry), Products (Consumables, Microplates, Biosensor Chips), Applications (Binding Kinetics, Binding Thermodynamics, Lead Generation) - Global Forecasts to 2020," USA, Jan 2016.

[2] M. Nagel, P. H. Bolivar, M. Brucherseifer, H. Kurz, A. Bosserhoff, and R. Buttner, "Integrated THz technology for label-free genetic diagnostics," *Applied Physics Letters*, vol. 80, pp. 154-156, Jan 7 2002.

[3] A. E. Grow, L. L. Wood, J. L. Claycomb, and P. A. Thompson, "New biochip technology for label-free detection of pathogens and their toxins," *Journal of Microbiological Methods*, vol. 53, pp. 221-233, May 2003.

[4] P. Estrela, A. G. Stewart, F. Yan and P. Migliorato, "Field effect detection of biomolecular interactions," *Electrochimica Acta*, vol. 50, pp. 4995-5000, Sep 2005.

[5] W. U. Wang, C. Chen, K. H. Lin, Y. Fang, and C. M. Lieber, "Label-free detection of small-molecule-protein interactions by using nanowire nanosensors," *Proceedings of the National Academy of Sciences of the United States of America*, vol. 102, pp. 3208-3212, Mar 1 2005.

[6] A. Kukol, P. Li, P. Estrela, P. Ko-Ferrigno, and P. Migliorato, "Label-free electrical detection of DNA hybridization for the example of influenza virus gene sequences," *Analytical Biochemistry*, vol. 374, pp. 143-153, Mar 1 2008.

[7] F. Vollmer and S. Arnold, "Whispering-gallery-mode biosensing: label-free detection down to single molecules," *Nature Methods*, vol. 5, pp. 591-596, Jul 2008.

[8] S. Sorgenfrei, C. Y. Chiu, R. L. Gonzalez, Y. J. Yu, P. Kim, C. Nuckolls, *et al.*, "Label-free single-molecule detection of DNA-hybridization kinetics with a carbon nanotube field-effect transistor," *Nature Nanotechnology*, vol. 6, pp. 125-131, Feb 2011.

[9] P. Estrela, D. Paul, P. Li, S. D. Keighley, P. Migliorato, S. Laurenson, *et al.*, "Label-free detection of protein interactions with peptide aptamers by open circuit potential measurement," *Electrochimica Acta*, vol. 53, pp. 6489-6496, Sep 20 2008.

[10] P. Estrela and P. Migliorato, "Chemical and biological sensors using polycrystalline silicon TFTs," *Journal of Materials Chemistry*, vol. 17, pp. 219-224, 2007.

[11] H.J.N.P.D. Mello, T. Heimfarth and M. Mulato, "Influence of the physical-chemical properties of polyaniline thin films on the final sensitivity of varied field effect sensors," *Materials Chemistry and Physics*, vol. 160, pp. 257-263, Jun 2015.

[12] S. V. Harb, S. H. Pulcinelli, C. V. Santilli, K. M. Knowles, and P. Hammer, "A comparative study on graphene oxide and carbon nanotube reinforcement of PMMA-siloxane-silica anticorrosive coatings," *ACS Applied Materials & Interfaces*, vol. 8, pp. 16339-16350, June 29 2016.

[13] J. G. Bruno, "Predicting the uncertain future of aptamer-based diagnostics and therapeutics," *Molecules*, vol. 20, pp. 6866-6887, Apr 2015.

[14] J. W. Lee, H. J. Kim, and K. Heo, "Therapeutic aptamers: developmental potential as anticancer drugs," *BMB Reports*, vol. 48, pp. 234-237, Apr 30 2015.

[15] T. Mairal, V. C. Ozalp, P. L. Sanchez, M. Mir, I. Katakis, and C. K. O'Sullivan, "Aptamers: molecular tools for analytical applications," *Analytical and Bioanalytical Chemistry*, vol. 390, pp. 989-1007, Feb 2008.

[16] S. Jeong, S. R. Han, Y. J. Lee, and S. W. Lee, "Selection of RNA aptamers specific to active prostate-specific antigen," *Biotechnology Letters*, vol. 32, pp. 379-385, Mar 2010.

[17] W. J. Catalona, D. S. Smith, T. L. Ratliff, K. M. Dodds, D. E. Coplen, J. J. J. Yuan, *et al.*, "Measurement of prostate-specific antigen in serum as a screening test for prostate cancer," *New England Journal of Medicine*, vol. 324, pp. 1156-1161, Apr 25 1991.

[18] D. A. Healy, C. J. Hayes, P. Leonard, L. McKenna, and R. O'Kennedy, "Biosensor developments: application to prostate-specific antigen detection," *Trends in Biotechnology*, vol. 25, pp. 125-131, Mar 2007.

[19] N. Savory, K. Abe, K. Sode, and K. Ikebukuro, "Selection of DNA aptamer against prostate specific antigen using a genetic algorithm and application to sensing," *Biosensors & Bioelectronics*, vol. 26, pp. 1386-1391, Dec 15 2010.

[20] P. Jolly, N. Formisano, J. Tkac, P. Kasak, C. G. Frost, and P. Estrela, "Label-free impedimetric aptasensor with antifouling surface chemistry: A prostate specific antigen case study," *Sensors and Actuators B*, vol. 209, pp. 306-312, Mar 31 2015.

[21] N. Formisano, P. Jolly, N. Bhalla, M. Cromhout, S. P. Flanagan, R. Fogel, *et al.*, "Optimisation of an electrochemical impedance spectroscopy aptasensor by exploiting quartz crystal microbalance with dissipation signals," *Sensors and Actuators B*, vol. 220, pp. 369-375, Dec 1 2015.

[22] S. K. Hong, "Kallikreins as biomarkers for prostate cancer," *BioMed Research International*, vol. 2014, art. 526341, Apr 1 2014.

Figure captions

Fig. 1 Schematic of the basic design of a single channel OCP measurement system. WE is the working electrode; RE the reference electrode; the Pt wire is grounding the solution.

Fig. 2 (a) An illustration of the whole OCP system setup, including the fabricated PSA aptasensor loaded in a flow cell. (b) A photo of the flow cell and circuit board.

Fig. 3 An illustration of the whole OCP system setup, including the fabricated PSA aptasensor loaded in a flow cell.

Fig. 4 A typical OCP behaviour of the aptasensor with the response of consecutive injections of different concentrations of PSA (black arrows) and rinsing buffer (blue arrows) on four separate electrodes of the array. The numbers next to the black arrows indicate the PSA concentrations injected. The inset shows the initialization of the OCP measurement with an injection of buffer (blank solution).

Fig. 5 Dose response of the aptasensor. The points represent the average for 4 channels. The line represents a linear fit to the points between 1 and 10 ng/ml (as shown in the inset using a linear scale).

Fig. 6 A comparison of response with blank, hK2 (100 ng/ml), HSA (66000 ng/ml) and PSA (100 ng/ml) fabricated sensors.

Figure for table of contents